

## 1.1 CEDAR

### 1.1.1 CEDAR Detector Requirements

The disadvantage of high energy protons used by NA62 and, consequently, of a high energy secondary beam, is that the kaons cannot be efficiently separated from pions and protons at the beam level. The consequence is that the upstream detectors which measure the momentum and the direction of the kaons are exposed to a particle flux about 17 times larger than the useful (kaon) one. A critical aspect is therefore to positively identify the minority particles of interest, kaons, in a high rate environment before their decay. This will be achieved by placing in the incoming beam a differential Cerenkov counter, CEDAR, filled with hydrogen gas.

originally CEDAR  
was filled with H<sub>2</sub>  
gas

A FLUKA simulation was used to study the interactions of pions, kaons and protons with the residual gas in the vacuum decay tank and the probability that such an interaction can cause fake triggers was computed. The conclusion is that (in the absence of kaon tagging) the vacuum should be better than  $6 \cdot 10^{-8}$  mbar to keep the background to less than one fake event per year. This very challenging requirement can be relaxed by at least an order of magnitude by positively tagging the kaons by means of a CEDAR Cerenkov counter in the beam line, filled with hydrogen gas at an absolute pressure of about 3.6 bar. A necessary part of this kaon identification is the precise timing of the different components in order to guarantee a good rejection of the background due to the accidental overlap of events in the detector.

An upgraded form of the CEDAR built for the SPS secondary beams (CERN Report CERN-82-13) will be used, and will be insensitive to pions and protons with minimal accidental mis-tagging. The choice of the Hydrogen gas is dictated by the need to minimise material on the beam line, and hence reduce multiple Coulomb scattering – see Table 1. The foreseen thicknesses of the upstream and downstream aluminium vacuum windows are 150 µm and 200 µm, correspondingly.

what is xsi\_0

Table 1: the thickness expressed in  $X_0$  for different gases used in the CEDAR counter. The pressure values are chosen to have the same index of refraction.

|                                       | Helium | Nitrogen | Hydrogen |
|---------------------------------------|--------|----------|----------|
| Pressure [bar]                        | 10     | 1.7      | 3        |
| Al window thickness [µm]              | 2x400  | 2x100    | 150+200  |
| Al window thickness [ $10^{-3} X_0$ ] | 9.0    | 2.2      | 3.9      |
| Gas thickness [ $10^{-3} X_0$ ]       | 12     | 35       | 3.2      |
| Total thickness [ $10^{-3} X_0$ ]     | 21     | 37       | 6.6      |

### 1.1.2 Overview of the CEDAR operation

The CERN CEDAR counter (see Figure 1) has been designed to identify particles of a specific mass by making the detector blind to the Cerenkov light produced by particles of different mass. For a given beam momentum, the Cerenkov angle of the light emitted by a particle traversing a gas of a given pressure is a unique function of the mass of the particle and the wavelength of the emitted light. The Cerenkov light emitted by particles of different mass is then not transported by the CEDAR optics through the diaphragm slit onto the light detectors but absorbed on its way, as explained in more detail below.

*Table 2: Characteristics and resolutions of the CEDAR*

for a general CERN CEDAR counter

| Parameter                  | Value                   |
|----------------------------|-------------------------|
| Gas type:                  | H <sub>2</sub>          |
| n-1                        | ~142 x 10 <sup>-6</sup> |
| Nominal pressure for kaons | 3.85 bar                |
| θK                         | 30.9 mrad               |
| Kaon rate                  | 50 MHz                  |
| Time resolution            | <100 ps                 |
| Δθ/θ                       | 4.8 10 <sup>-3</sup>    |
| Δβ/β                       | 5x10 <sup>-6</sup>      |
| Number of photons per kaon | 100                     |
| Rate per photomultiplier   | 3 MHz                   |

The CEDAR consists of a pressure vessel filled with gas of a precisely controlled pressure. At the end of the vessel, the Cerenkov light is reflected by a spherical Mangin mirror onto a ring-shaped diaphragm of 100 mm radius with adjustable aperture width, located at the beginning of the vessel. The pressure of the gas can be adjusted so that only light of the wanted particle type will be transmitted through the diaphragm slit. Eight photomultipliers in its original version are placed behind the slit and the coincidence of at least 6 of them will indicate the passage of a particle of the wanted mass. A chromatic corrector lens, designed to match the dispersion curve of the gas and positioned in between the mirror and the diaphragm, ensures that the light of all wavelengths arrives at the same radius on the diaphragm plane. The advantage of this design is that light from unwanted particles hits the diaphragm plane at a different radius from that of wanted particles. It therefore does not pass through the aperture and does not contribute to the rate. Hence the device is well suited to tagging minority particles in a high-intensity beam. This only works if all rings are concentric, which requires all beam particles to be parallel to each other. This imposes certain constraints on the beam optics.

description of  
the picture  
below

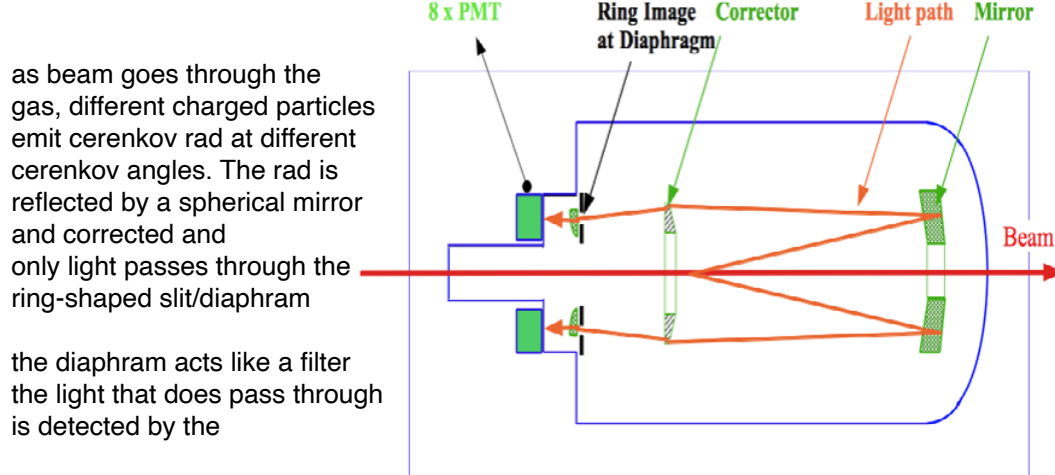


*Figure 1 Schematic layout of the Standard West-Area CEDAR.*

Two versions of the CEDAR counter have been built for use at the SPS (1). The North CEDAR, filled with Helium gas, is optimized for high energies and the West CEDAR, Nitrogen filled, for lower beam momenta. The difference is related to the Cerenkov angle, determined by the beam momentum and the refractive index of the gas, and the optical correction, which relates to the dispersion of the gas used. It has been verified by a ray tracing program that the West version of this instrument would function well for our application using Hydrogen at room temperature instead of Nitrogen, thus reducing significantly the scattering of the beam in the gas. The optical design minimises the dispersion of Cerenkov light and enables the aperture of the diaphragm to be reduced. Thus, photons produced by charged kaons pass through while light from pions and protons is blocked. During 2006, a test run was performed on one of the CEDAR-West Cerenkov counters (filled with N<sub>2</sub>) and validated its ability to distinguish kaons from pions and protons in the NA62 experiment, as well as the light spot shape predicted by a simulation program. It was also found from the simulation that the upstream 1.2 metre section of beam pipe containing hydrogen contributes only marginally to the efficiency and can thus be replaced by an extension of the beam vacuum pipe. In addition to a small reduction in multiple Coulomb scattering, such a modification is helpful in the redesign of the optical system necessary to handle the increased photon flux. The main parameters of the proposed Hydrogen-filled CEDAR-W counter are listed in Table 2.

The main effects that broaden the light spot at the diaphragm are:

1. optical aberrations, limited to about 6 microns and therefore negligible;
2. chromatic dispersion, largely corrected for by the chromatic corrector;
3. multiple scattering of the beam during its traversal of the gas, minimised by the choice of Hydrogen gas;

4. inhomogeneity of the refractive index of the gas due to temperature gradients, minimised by thermal insulation and (in the case of NA62) by the location of the CEDAR in an underground area with inherently rather stable temperature;
5. beam divergence, which is one of the dominant factors, but limited to an RMS angle of about  $70 \mu\text{ rad}$  in each plane according to full beam transport simulation;
6. noise and halo particles contributing to the scintillation light produced in the gas.

The rate from the kaon component in the high-intensity beam for NA62 is 50 MHz and the size of the light spot emerging from each quartz window is  $30 \times 8 \text{ mm}$  (rectangular). The CEDAR detector is required to achieve a kaon tagging efficiency of at least 95%, with a time resolution of 100 ps. The present photomultipliers are too slow for this purpose, and an optical system with appropriate and multiple photodetectors will be developed to achieve a singles rate on each pixel not higher than 3 MHz mm<sup>-2</sup>.

requires KTAG

### 1.1.3 CEDAR West: Vessel and internal optics

The CEDAR counter is housed in a steel pressure vessel of 534 mm inner diameter and 558 mm outer diameter, welded on square flanges, to which a nose with eight quartz windows is bolted on the upstream end while a spherical head closes the downstream end. The overall length of the main vessel is 4500 mm. A 1243 mm long nose extends upstream of the quartz windows making the overall length of the counter 6200 mm. The thermal expansion is 0.05 mm/K. The beam windows at the entry and exit are 100 mm diameter, and made out of Aluminium alloy. The measurement of 6200 mm quoted above includes the thermal shielding and external envelope, while the value 5772 mm refers to the length of the gas volume including the full nose. The dimensions of the shortened counter are being decided, including shielding and infrastructure. There is also some length required for the diaphragm window. (See the overall drawing at url: <http://na48.web.cern.ch/NA48/NA48-3/groups/beam/CEDAR/CedarDrawing.pdf>).

*Table 3: Relative positions of all optical elements with respect to the entrance window*

| Element                          | Z (mm) |
|----------------------------------|--------|
| Entrance window                  | 0      |
| Upstream end of quartz windows   | 1111   |
| Condenser plane                  | 1211   |
| Diaphragm plane                  | 1251   |
| Chromatic corrector upstream end | 2234   |
| Mangin mirror exit               | 5772   |
| Exit window                      | 5772   |

The optical elements inside the counter comprise the mangin mirror, the chromatic corrector, the diaphragm and 8 sets of condenser lenses and quartz windows. A sketch of the overall layout and

the optical path is given in Figure 2 and the relative positions of all elements with respect to the entrance window are listed in Table 3.

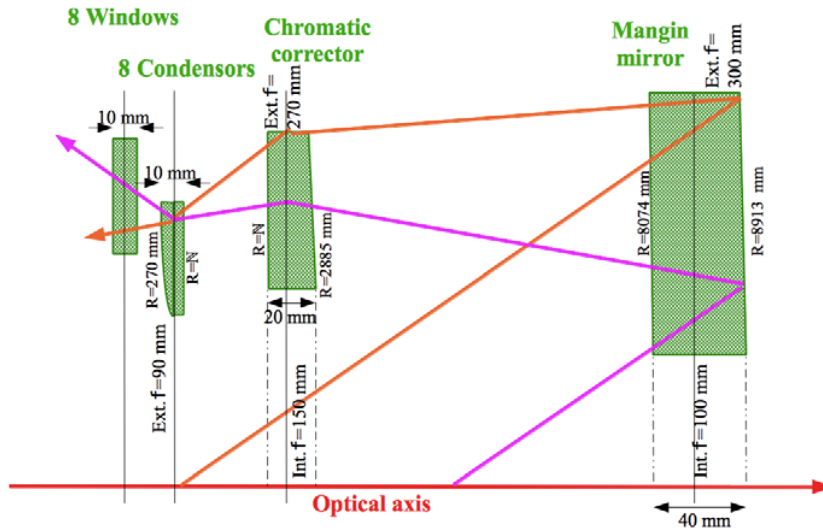


*Figure 2: Schematic layout of the optical elements and the light path.*

The whole counter is packed with 100 mm of polyurethane foam to provide thermal insulation and this ensures a temperature uniformity of  $\pm 0.1$  degrees. The supporting feet, gas pipes and electric cables are designed to minimise thermal conduction to the outside world. Furthermore, thick Aluminium shells have been clamped to the outside of the big vessel and Copper shells are fastened on the nose. These modifications enable the impact of external temperature variations to be reduced by a factor of about 20. The vessel temperature is monitored by three platinum wire thermometers located at both ends and at the diaphragm plane.

The optical axis of the CEDAR counter must be precisely aligned with the beam axis. To that end the vessel is supported in three points. One point is fixed and located at the longitudinal position of the quartz windows. The two other points are located 4.347 m downstream and rest on a V-shaped surface under the mirror. The alignment system, made of cast Aluminium, has two chariots moved by right-left screw drive, opening the V-surface. By moving the chariots in opposite direction the vertical position can be adjusted, whereas another screw drive allows a motion in the same direction and thus a horizontal adjustment. The step resolution is 10 microns providing an angular positioning within  $\pm 2.3 \mu$  rad. The X, Y range is from -4.3 to +4.3 mm.

The optical elements (mangin mirror, chromatic corrector, and diaphragm) are attached to an optical tower made as an isostatic, triangular assembly of tubes bolted onto spherical cups. This tower is straight to within  $\pm 0.2$  mm over 4.5 metres and has a static sag of 0.1 mm. It is supported by a sphere under the diaphragm and is fixed without constraint to the pressure vessel so that pressure and temperature variations do not affect the optical axis. The ring diaphragm is fixed at the upstream end of the tower. The mirror is located at the downstream end and can be aligned in radial

and longitudinal directions. The chromatic corrector rests on the first intermediate ring of the tower and can be aligned in three directions.

The mangin mirror is made from high-quality Suprasil I quartz blanks. The outer diameter is 300 mm, the diameter of the inner hole is 100 mm. The thickness of the quartz mirror is 40 mm, with different radii of curvature for the reflecting surface, 8610 mm, and the refracting surface, 6615 mm. Lens and mirror surfaces were polished to give an optical path length homogeneous to the required  $\lambda/8$ . The figures quoted here are CEDAR-W, as used in the design. The dimensions quoted in Figure 2 are relative to the CEDAR-N, and should be taken only as an example.

The chromatic corrector is also made out of Suprasil I of 20 mm thickness. The outer diameter is 320 mm and the diameter of the hole 150 mm. The radius of curvature of the entrance surface is 1385 mm, while the exit surface is flat ( $R > 5000$  km).

The 8 optical windows are made of quartz cylinders of 45 mm diameter and 10 mm thickness. Their ring frame is made of stainless steel and the binding is obtained by heating the rings at 150°C. A layer of Silver was deposited on the circumference of the quartz disk before heating. After cool-down the silver layer is compressed and produces a perfect seal. In a destructive test, a pressure of 300 bar was reached.

All optical surfaces are coated with a quarter-wavelength thickness of MgF<sub>2</sub> for minimum reflection at 300 nm wavelength.

The diaphragm comprises a disk with 8 elongated apertures and 8 outer and inner segments moved by right-left screw drives. The segments are bolted onto high-precision guided chariots. The 8 screw drives are provided with gears and are turned simultaneously by a gear mounted on ball bearings in a V-groove on the periphery of the disc. The opening can be varied between 0.03 and 20 mm in steps of 0.01 mm with a motor located external to the vessel. The circularity of the aperture shows radial deviations below 0.02 mm. The azimuthal opening of the diaphragm is 8 times 42.6 degrees and covers 95% of the ring.

### 1.1.4 Adapting the CEDAR for NA62

NA62 will use the West CEDAR filled with hydrogen at up to 5 bar (note: up to 5 bar for pressure scans is needed to see full proton peak). The nose will be shorten from 1243 mm to about 600 mm. The design of the mechanics and cooling system must accommodate the different potential choices of the optical readout system, minimise the flux of muons and neutrons hitting the photo-detectors, and ensure high levels of optical efficiency and stability, as well as minimising temperature gradients in the vicinity of the CEDAR. New photodetectors and associate electronics are needed in order to operate at the required kaon rate. A detailed description of the necessary changes and adaptations is given in the following sections.

### 1.1.5 Light transport system

The optics of the CEDAR light collection must be re-designed to match the photodetectors necessary to handle the high beam flux in NA62. Reflecting the light through 90 degrees will also be necessary to allow the greater space required for photodetectors and preamplifiers and to locate them so as to

minimise damage from radiation. The final design of the light collection system is highly correlated with the technology choice for the photodetectors, with different rate, noise limitations and packing density. As a consequence the light may have to be focussed or de-focussed onto the photodetector planes using ellipsoidal mirrors as illustrated in Figure 3 and a lensing system to focus the light onto the active area of the photodetectors.

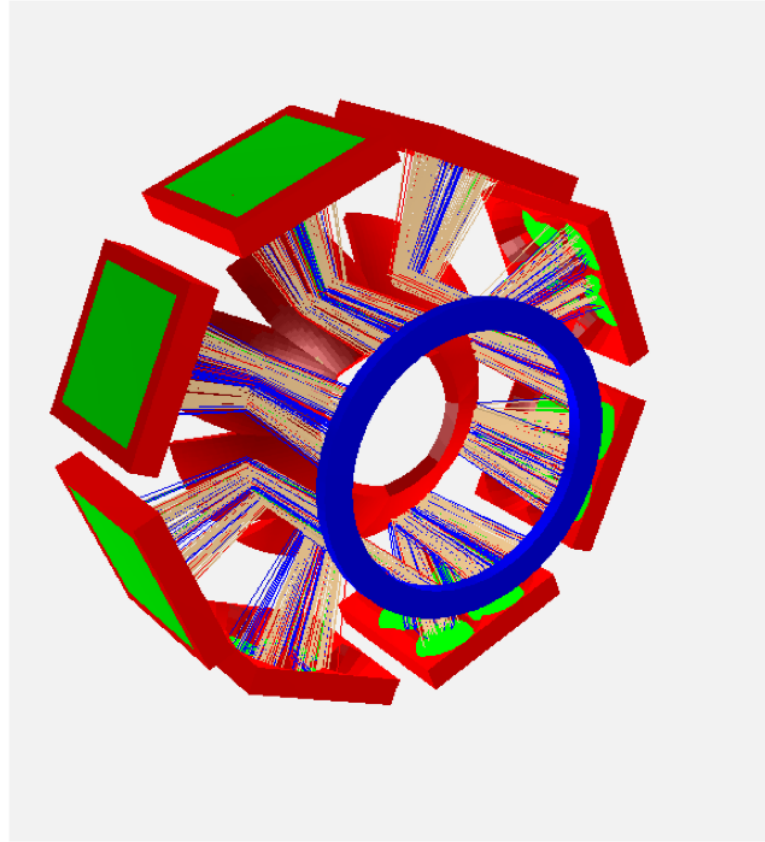


*Figure 3: The Simulation of 100 events in the CEDAR nose cone. The ray tracing of the photons from (right to left) the quartz window (blue), the ellipsoidal mirrors (red), the light collection cones (red) and photodetector plane (green) is illustrated. The optical components are schematic and do not reflect a final geometrical arrangement. The photons are shown in fawn for those that are detected directly and blue if detected after reflection from the cone. Photons that are lost at reflection in the cone are shown in green whilst those photons lost by reflection at the PMT window are indicated in red.*

One possible solution, adopted by the NA62 RICH detector, would be the use of light-collection cones. Again, the final design of such light collectors is dependent on the choice of photodetector technology. A proof of principle of the full optical system has to be developed for each of the photodetector options. Initial simulation studies have been undertaken to understand the design of the optical components. These preliminary studies indicate that the depth and design of the light-collection cones will be critical. A cone design that is too shallow will result in loss of photons at the phototube window due to Fresnel reflection and will suffer from light being reflected back out of the cone. With a cone that is too deep difficulties could arise in the manufacture process to ensure a

good reflective coating. The preliminary studies indicate that a photon collection efficiency of ~90% should be achievable. This design study assumed ellipsoidal collection cones, with a depth between 10-25mm; a conical design is currently under investigation. The simulation of 100 events overlaid is shown in Figure 3, the photons are generated via a full simulation of the CEDAR.

The mirrors will be fabricated from glass with radii of curvature of the ellipsoidal sections still to be optimised. The light collection system will be a bespoke solution with two approaches under consideration: machining the “cones” out of a solid block, or creating a mandrel and manufacturing the cones out of plastic, glass or carbon fibre. Further studies are in progress to ensure that the light losses in the cones due to reflections and non-normal incidence are kept to a minimum, acceptable level.

### 1.1.6 Mechanical Support, Cooling and Safety Considerations

The major mechanical considerations involved in modifying the Frontend of the CERN West CEDAR for use by NA62 are as follows:

- The photodetectors and optical components must be redesigned and located to maximise the capture of Cerenkov light, and mechanical rigidity must ensure optical stability.
- The preamplifiers and signal-shaping electronics must be located adjacent to the photodetectors with signal-processing electronics removed from hazardous radiation.
- The existing protective and thermally-insulated metal cover around the nose section of the CEDAR must be replaced. Cooling and insulation must be designed to minimise temperature gradients and thermal instability that might result in unacceptable local variations in the refractive index of the hydrogen gas.

The safety requirements resulting from the necessary mechanical modifications and the use of hydrogen gas are as follows:

- A nitrogen blanket around the optical-readout electronics and HV is required to eliminate any possibility of an explosion in the event of a hydrogen leak from the CEDAR. The mechanical design will incorporate sensors to monitor the flow of nitrogen and the temperature of the enclosure, as discussed below in the gas and safety sections.
- The CEDAR must be connected to the vacuum beam pipe at both ends in such a way that a hydrogen leak is not accompanied by any admixture of air in order to prevent any risk of explosion. An important secondary consideration is that damage to sensitive detectors must be minimised by mitigating the effects of hydrogen leaks and the shock wave resulting from the potential rupture of the window at either end of the CEDAR. The proposed way of doing this involves a single aluminium window between the high-pressure hydrogen and vacuum beampipe at each end of the CEDAR with a large vacuum volume to capture any escaping hydrogen. This task is being studied by the Beam group and is now completely separate from any modifications to the CEDAR nose. A preliminary schematic drawing of the pressure protection volume is shown in Figure 5.

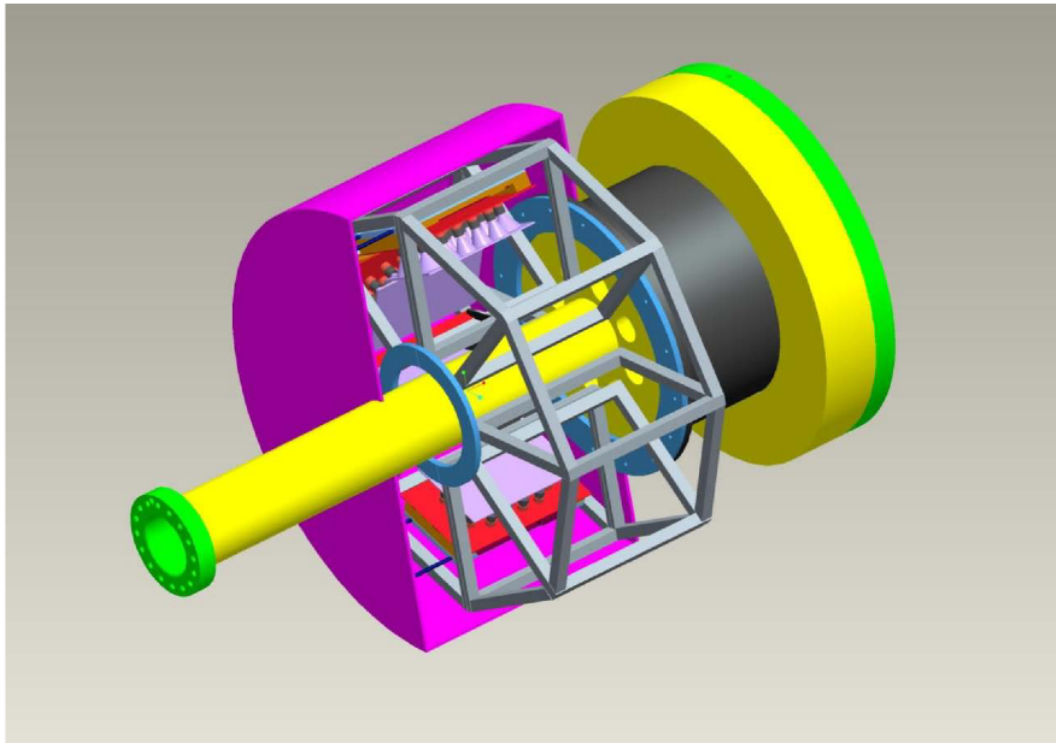


*Figure 4: Conceptual Design of the Support Structure and Nitrogen Enclosure.*

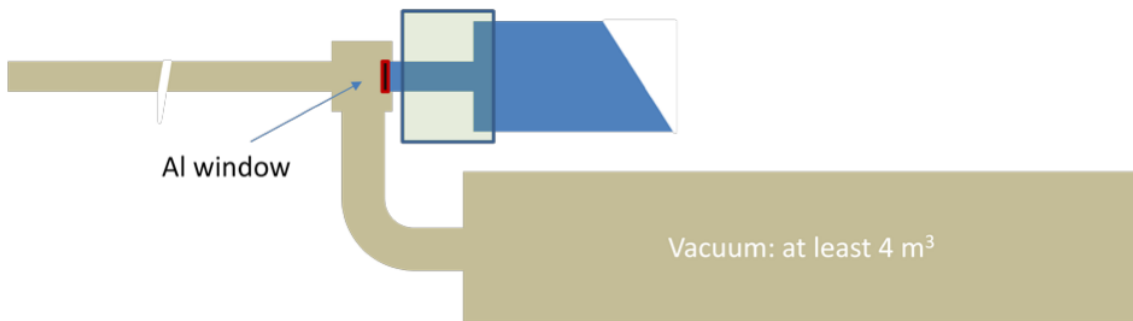


*Figure 5: Conceptual drawing of the retention vacuum volume attached to the upstream end of the CEDAR( in blue). The aluminum window on the upstream side has thickness of 150 µm, the downstream window has a thickness of 200 µm.*

#### 1.1.6.1 Adapting the existing CEDAR nose

The proposed design involves replacing the current photo-detection system of 8 PMT's and the protective and thermally-insulated metal cover forming the front end of the CEDAR. All optical components internal to the CEDAR are already optimised for use with hydrogen, while the seals on the quartz windows are perfectly safe for use with hydrogen at 5 bar.

Because of their increased size and unavoidable dead space the 8 new sets of photo-detectors will need to be relocated away from the quartz windows in the nose, and light guides will be required to focus the Cerenkov light onto their active surfaces. The mechanical challenge is to preserve the current optical stability and ensure that all the Cerenkov light reaches the photo-detectors. This requires the precision mounting of the photo-detectors and optical components in a rigid, light-weight structure that can be precisely located relative to the quartz windows of the existing nose.

A disc-shaped lattice support structure housing the new photodetectors, optics, readout electronics and cooling will be cantilevered off a support cylinder bolted onto the CEDAR flange. This structure will support all cabling and cooling pipes and be enclosed in a gas-tight environmental chamber through which Nitrogen gas will be circulated. A separate protective metal cover [not shown] will enclose the environmental chamber and clip onto the metal cover enclosing the main body of the CEDAR.

In addition to removing the heat from the electronics it is important to maintain a constant temperature for all components of the CEDAR nose that are in thermal contact with the hydrogen gas in order to prevent local variations in density that will affect the refractive index. This will be done by a combination of heat removal, using chilled de-ionised water, and thermal insulation. Finally, it is important that the design ensures rapid access to, and replacement of, any PMT or electronic component that may fail during use.

#### 1.1.6.2 The Photodetector Support Structure

Our conceptual design locates the 8 sets of photo-detectors and readout electronics into 8 pods within a lightweight, disc-shaped latticework support structure at a radius of about 30 cm from the beam. Studies indicate that the high-intensity neutron background radiation is rather uniform and that it will not be necessary to vary the radius or azimuthal angle of any of the 8 pods. A customised, ellipsoidal 45° mirror to reflect the Cerenkov light from each of the 8 CEDAR quartz windows towards a set of photo-detectors will be located at the same radial position as the quartz window. A set of light guides, using either internal reflection from Plexiglas (male) cones or reflection from the surfaces of polished metal (female) cones, will channel the light onto the active surfaces of the photodetectors. The cones will be designed with variable light-collection areas to ensure approximate equalisation of the light intensity falling onto each PMT. Provision will be made for fine adjustments to the position and angles of the mirrors.

The photodetector support structure will be built in two halves that can be ‘clam-shelled’ around the beampipe and precisely located onto the support cylinder to facilitate installation. Figure 6 shows a cross-section of one half of the support structure with the envisaged layout of optical and electronic components and cooling plates. The cooling pipes and cabling [not shown] will be led around the outside of the structure and out of the environmental chamber to the floor, where appropriate patch panels are situated. Both the support cylinder and support structure will remain fixed in place after installation and the optics and electronics in each of the 8 segments will be mounted in drawers that slide forwards to enable access to the relevant components through the environmental chamber.

We envisage a separate, nitrogen-flushed, environmental chamber, made in two sections from lightweight carbon fibre, which surrounds the support structure and is supported off it. Simple non-

load-bearing seals around the beam pipe and support cylinder will ensure the necessary degree of gas-tightness. Ports will be incorporated to enable rapid nitrogen flushing to remove air from the system and to relieve excessive overpressure. The front face of the chamber will incorporate removable panels to enable rapid access to the electronics, cooling and optics within each sector. This chamber will also ensure that no extraneous light enters the optical system and will keep out any dust. The whole structure will be covered by a protective metal casing rigidly clamped to that of the main CEDAR. This casing will have front doors that can be removed or opened to enable unrestricted access to the front of the environmental chamber and hence to all components within the support structure.

The thermal environment must be controlled to ensure that the hydrogen gas in all parts of the CEDAR remains at a constant temperature and that any changes in temperature occur only very slowly and without local fluctuations. To this end the insulation within the protective cover surrounding the main body of the CEDAR will be upgraded with better performing, fire-retarding material. Thermal design of the new CEDAR Frontend will concentrate on removing the heat generated by the electronics and insulating those surfaces in thermal contact with hydrogen gas or with the main body of the CEDAR. The three regions that require particular attention are: i) the hydrogen-filled beampipe; ii) the curved surface and front face of the nose in which the quartz windows are situated; and iii) the flange onto which the support cylinder is bolted. Purpose-designed insulation will be incorporated into these different areas, as indicated in yellow in Figure 4. Details of the proposed temperature control and monitoring are given in section 1.1.6.3.

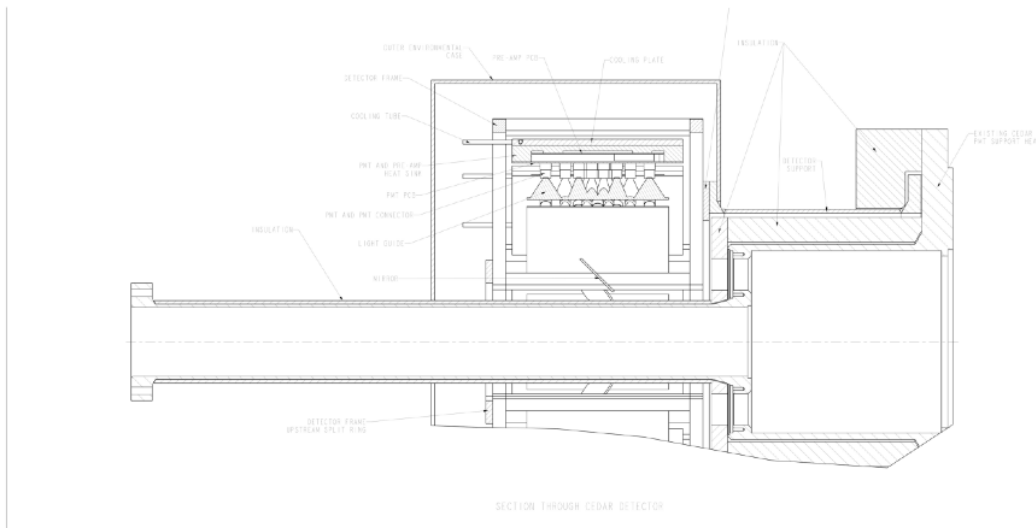


*Figure 6 : Cross-sectional Layout of the Support Structure and Nitrogen Enclosure*

An installation frame will be required to hold the two halves of the support structure as they are populated with optical, electronic and cooling components in the laboratory and to facilitate system tests prior to installation on beamline. It is likely that this frame will also be useful in supporting the two halves of the structure while they are being bolted to the support cylinder after being craned

onto the beamline and in facilitating the location of the environmental chamber. It is envisaged that the outer protective metal casing will be craned directly into place.

### **1.1.6.3 Safety Considerations, Cooling and Monitoring.**

All custom made electrical equipment on the detector (photodetectors and electronics) will be enclosed within the environmental chamber that is filled with dry nitrogen gas to prevent the development of an explosive atmosphere in the event of hydrogen leaks. A small overpressure will ensure that a nitrogen atmosphere also surrounds the optical components in the support structure and prevents any possibility of moisture condensing from the atmosphere. If the nitrogen pressure drops, the power will be cut to the photodetectors and readout electronics to prevent the occurrence of any sparks within the enclosure.

The heat load from the photodetectors and front-end electronics is not expected to exceed 10 W per sector, or 100 W in total. This heat will be removed as near to source as possible by metal cooling plates, through which chilled de-ionised water flows, in thermal contact with heat sinks on the electronics PCBs. The temperature and flow of water through the cooling manifold will be controlled by electronics monitoring the temperature difference between the hydrogen beampipe close to the nose and that of the main body of the CEDAR and also the rate of change of temperature within the gas enclosure. The aim will be to maintain a stable temperature at the beampipe within  $\pm 0.1^\circ\text{C}$ .

It is important to monitor the long-term performance of the  $45^\circ$  mirrors and Light Guides in case any of the surfaces should deteriorate. Early warning would enable replacement parts to be fabricated in good time. A system of 8 ultra-violet LEDs will be installed on the CEDAR nose symmetrically spaced between the 8 quartz windows. By flashing the LEDs and monitoring the output from the 8 groups of photo-detectors the overall response of the optical and electronic systems may be monitored. Factoring out the response of the electronics and photodetectors, obtained from separate monitoring, will provide a long-term record of the optical performance of all parts of the system to enable early warning of any deterioration of the optical components. Careful design is necessary to enable separation of the different contributions from the mirrors and light guides, requiring more than one signal from each group of PMT's.

All custom-designed electronics will require certification by CERN for flammable safety and all commercial sensors will need an ATEX certificate for zone 2 (non-sparking) equipment.

### **1.1.7 Gas system**

Hydrogen gas has been identified as the most suitable radiator gas to operate the CEDAR detector. Physics performance arguments reveal two basic motivations for this choice:

- The use of Hydrogen limits the radiation length of the gas to 0.2 % of  $X_0$  (instead of 3% for Nitrogen or 1% for Helium).
- The refractive index, its wavelength dependence and the optical properties of the gas must be suitable to provide 95% efficiency for the identification of 75 GeV/c momentum kaons.

This gas is very flammable and must not mix with Oxygen (or Air) in any place of the system. All zones exposed to the gas system will be declared as flammable gas areas (Zone 2) and all equipment used in these areas must follow the CERN flammable gas safety rules.

All exhaust gases lines must be connected to the gas extraction system in TCC8.

### 1.1.7.1 Outline of the Gas System Design

The Hydrogen gas supply is located in the gas surface building 920, all other gas system components are situated in the experimental area (TCC8) close to the CEDAR detector itself. The relevant detector and gas-system parameters are summarized in Table 4.

*Table 4: Detector and gas system parameter*

|   |  |
|---|--|
| Radiator gas volume                         | 1.1 m <sup>3</sup>                       |
| Operating gas                               | 100% H <sub>2</sub>                      |
| Operating pressure                          | Between 2.5 and 3.5 bara <sup>1</sup>    |
| Pressure scans                              | Vary pressure in small steps around peak |
| Smallest pressure step during pressure scan | 5 mbar                                   |
| Absolute pressure (density) accuracy        | << 0.1%                                  |
| Detector leak rate                          | < 5.0 * 10 <sup>-4</sup> Std. cc/s       |

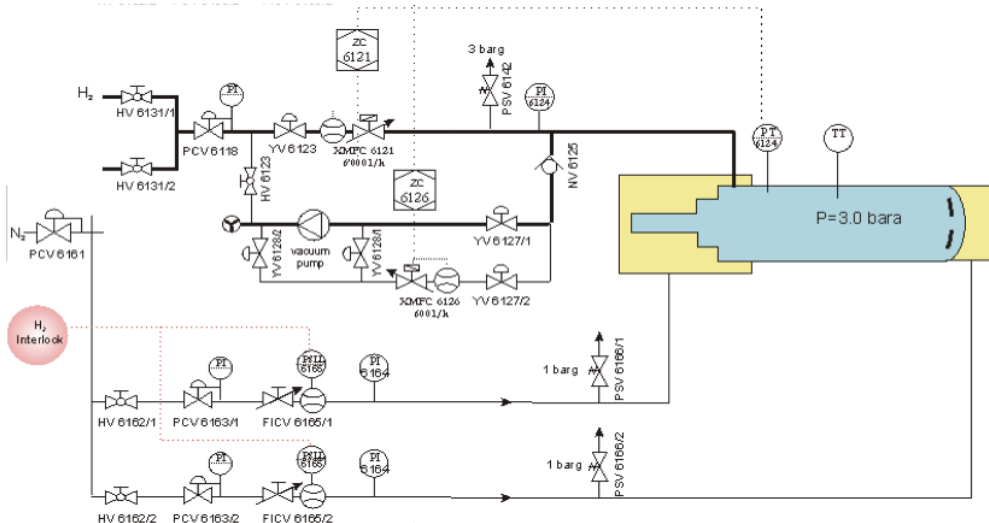


*Figure 7: Layout of the CEDAR gas system (blue = CEDAR radiator volume, yellow = envelope volumes)*

<sup>1</sup> The unit bara is used to denote that the scale refers to an absolute pressure referenced to vacuum.

The CEDAR radiator comprises a gas volume of about  $1.1 \text{ m}^3$ , which will be pressurized during operation to a constant pressure to detect kaons ( $\approx 3.6 \text{ bara}$ ). Unlike other gas systems, Cherenkov radiators do not need gas circulation; they can in fact operate with a fixed amount of gas without any gas renewal. This concept is advantageous because gas turbulence and temperature variations inside the detector will in this case not influence the gas density, providing temperature gradients are minimised.

The CEDAR gas system is shown in Figure 7. The input and output gas is metered using mass-flow-controllers, the absolute pressure inside the radiator is measured by means of a high accuracy transmitter, which has an absolute precision of 0.01% of full scale. The gas pressure and flows are monitored and controlled by a programmable control computer (PLC) allowing remote filling or emptying of the detector to any desired pressure. For safety reasons, some external parts of the detector will be enclosed by envelope volumes and be flushed with Nitrogen gas evacuating any Oxygen in the direct vicinity of the detector. In case of insufficient  $\text{N}_2$  flow the Hydrogen fill flow will be interrupted.

### 1.1.7.2 Filling and Emptying of the Detector

Before introducing any  $\text{H}_2$  gas, the entire system (including the detector) is filled with clean and dry  $\text{N}_2$  gas to evacuate air from the system. The detector is then pumped to vacuum using a dry membrane vacuum pump. If the detector has reached a vacuum pressure below 5 mbar the Hydrogen gas can be admitted to the detector and be filled to the desired pressure. At the end of a physics run the Hydrogen is pumped out and the detector is refilled with nitrogen.

### 1.1.7.3 Running mode and Pressure Scan

During physics operation the radiator pressure will be set accurately to the desired operation pressure, e.g. 3.73 bara. The gas density is then left constant by closing all valves to the radiator volume. To guarantee sufficient stability for long physics runs the leak rate of the detector must be smaller than  $5.0 * 10^{-4} \text{ Std. cc/s}$ . If this leak tightness cannot be reached the system can be upgraded with a density feed-back loop, so that the gas system compensates the gas losses automatically.

It is foreseen to perform pressure scans at regular intervals to calibrate the detector response around the kaon peak. To do this, the chamber pressure is varied in small steps ( $\Delta p \geq 5 \text{ mbar}$ ) between two limits to determine precisely the pressure with the highest counting rate for kaons. To maintain the best possible temperature stability, the pressure scan starts at the highest pressure and releases successively small amounts of gas from the detector.

### 1.1.8 Photodetectors

The CEDAR detector is required to achieve a kaon tagging efficiency of at least 95%, with a time resolution of 100 ps/kaon. The intrinsic rate due to the kaon component of the beam is approximately 50 MHz, and each kaon produces an average of 100 photons at the exit of the quartz window (i.e. losses due to internal mirrors and lenses are already included). The light spots produced by the CEDAR optics are a set of eight  $30 \times 8 \text{ mm}^2$  rectangular areas at the position of the quartz exit

windows, as illustrated in Figure 8. These photons will be guided onto the active surfaces of the photodetectors, as described earlier.

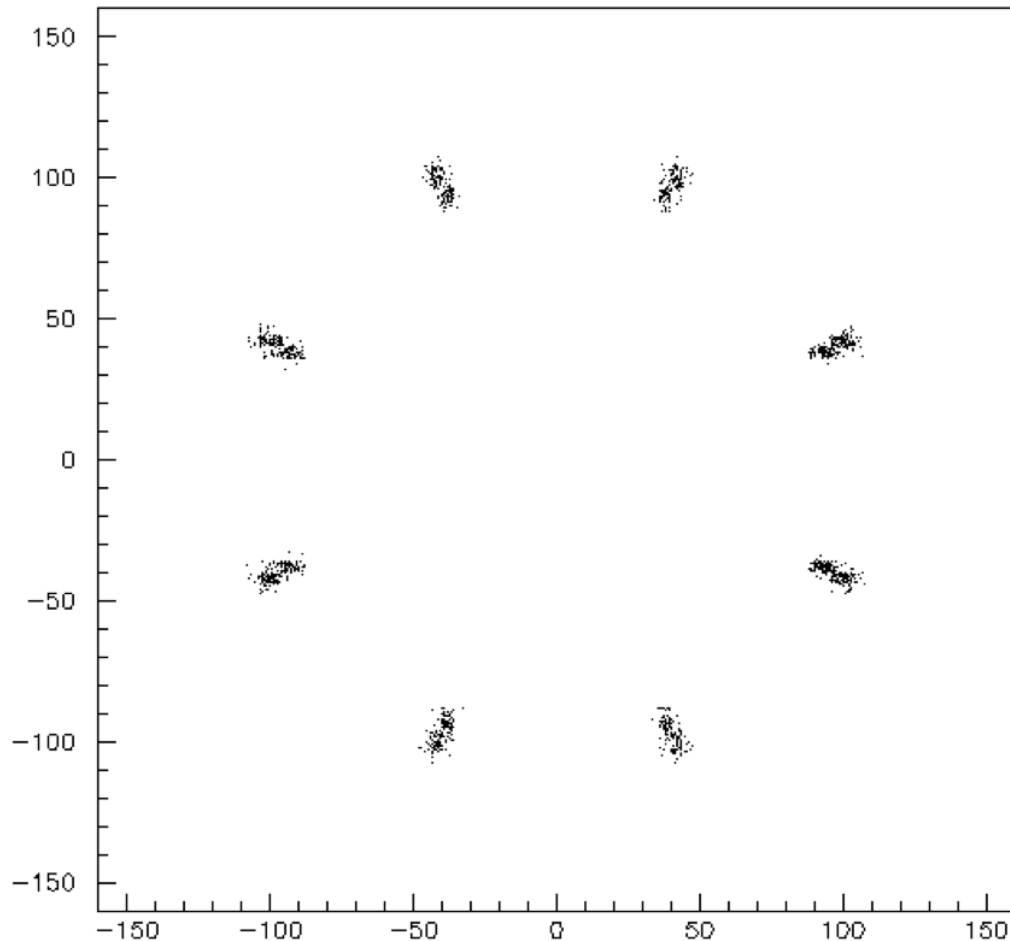


*Figure 8: Distribution of photons on the 8 quartz windows at the exit of the CEDAR*

At present the baseline choice of photodetector to be used for the CEDAR readout is conventional photomultipliers, particularly of the type used for the RICH detector: Hamamatsu R7400U-03. The number of photomultipliers will be chosen to maximise the kaon efficiency, while minimising the dead time and accidental noise.

Current technology limits the mean rate of single photons that can be detected efficiently by a detecting surface to be of the order of  $4 \text{ MHz mm}^{-2}$ . Assuming a photodetector with a gain of  $10^6$  and a quantum efficiency of 25% at the peak for  $\sim 420 \text{ nm}$  ( $\sim 20\%$  average), this would correspond to an equivalent anode current of  $0.1 \mu\text{A mm}^{-2}$ .

The light impinging on a spot is not uniformly distributed but is concentrated in the centre of the spot, as shown in Figure 8. However, if 30 PMTs are used to cover the spot, the hottest region will experience a rate of 4-5 MHz per PMT, which is within the PMT tolerance.

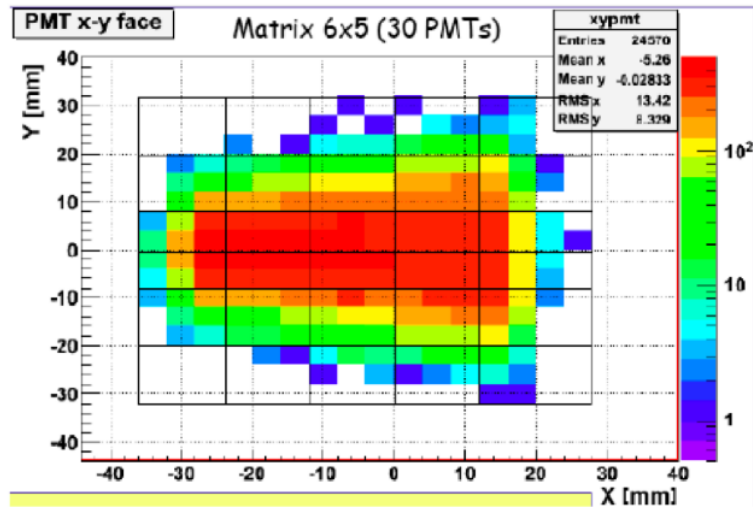


*Figure 9: Distribution of photons on 1 window at the exit of the CEDAR*

With 100 photons/kaon distributed among 8 spots, there are an average of 24 photons when convoluted with the quantum efficiency as a function of the wave length. Therefore an average of 3 photo-electrons per spot would be detected for a typical detection efficiency of 20%. For a typical photo-detector time resolution of 300ps the single kaon crossing time would therefore be measured with a resolution of  $300\text{ps}/24 = 60\text{ps}$ . When taking into account ~80% efficiency for additional lenses, mirrors and cones, the kaon detection efficiency with 3 photo-electrons/spot and a coincidence of various spots should easily exceed the required 95%. The coincident detection of photons will also address concerns about the effect of PMT thermal noise.

different design options

Vacuum photomultiplier tubes have a high resistance to damage by radiation and a relatively low dark-count rate. In addition PMT's with quartz windows are sensitive to short wavelengths. The large sensitive area simplifies the optics, since the sensitive region of each PMT is large enough that light collection cones can be used to channel the light, thereby reducing the effect of dead areas and making optimal use of the quantum efficiency. However the required combination of ~100 pico-second timing, high rate and long service life push the requirements to the limit of what is currently possible. Careful evaluation of other vacuum PMT options will be necessary, as well as an optimization procedure to establish the minimum number of PMT's necessary to achieve the desired performance.

Other options that could be considered are a single micro-channel-plate (MCP) photomultiplier and traditional multi anode technology. Table 5 lists some of the characteristics of the different PMT options. All devices have quartz, or UV-glass, faceplates with a short wavelength cut-off of approximately 160nm, or 185nm, respectively, and a quantum efficiency peaking at about 420nm.

The R5900 device is also available with an "Ultra Bialkali" photocathode with a peak quantum efficiency of 43% at 330nm.

*Table 5 Comparison of alternative phototube options with respect to the Hamamatsu R7400P (first row).*

| <b>Design Option</b>        | <b>Tube</b>             | <b>PMT per port</b> | <b>TTS (FWHM)</b> | <b>Peak QE</b> | <b>Peak <math>\lambda</math></b> | <b>Max anode current per device</b> | <b>Nominal Gain</b> | <b>Anode per device</b> |
|-----------------------------|-------------------------|---------------------|-------------------|----------------|----------------------------------|-------------------------------------|---------------------|-------------------------|
| Array of single-anode PMT's | Hamamatsu R7400P        | 30                  | 280ps             | 18%            | 420nm                            | 100 $\mu$ A                         | $10^6$              | 1                       |
| Multianode PMT              | Hamamatsu R5900U-00-L16 | 8                   | 180ps             | 21%            | 420nm                            | 100 $\mu$ A                         | $4 \times 10^6$     | 16                      |
| Multianode MCP-PMT          | Photek PMT240-96        | 1                   | 100ps             | 15%            | 420nm                            | 1.0 $\mu$ A                         | $2.5 \times 10^5$   | 96                      |

Using a multi-anode device would reduce the count rate on each channel and avoid issues with inefficiency due to pile-up. With 8 multi-anode PMT's, a photo-cathode quantum efficiency of  $\sim 25\%$  and a gain of  $\sim 10^6$  the total anode current will be approximately  $\sim 3 \mu\text{A}$ , well within the  $100 \mu\text{A}$  limit. *To verify the real gain of this device, more studies would be advisable.*

Microchannel plate PMT's offer high timing accuracy and fast rise times. Transit time spreads of  $\sim 30$  ps have been reported for single anode devices, although the response time for multi-anode device is  $\sim 100$  ps; the multianode device is also current limited. The response of MCP-PMT's is not linear, however, and there are local dead-spots after a pulse as the MCP recharges. Careful investigation of gain with pulse rate would therefore be needed. A MCP lifetime can be expressed in terms of  $\text{C}/\text{cm}^2$  and is typically about  $\sim 1 \text{ C}/\text{cm}^2$ . However, a tube from Photonis has been shown to give a significant reduction in gain after only  $0.4 \text{ C}/\text{cm}^2$ . The annual requirements from NA62 are  $\sim 3 \text{ C}/\text{cm}^2$ , well in excess of the expected limitation. It is known that this limit can be increased significantly using thin film fabrication techniques. The lifetime of any proposed MCP-PMT would have to be evaluated, especially since the PDE (typically 15%) is rather low and any reduction due to aging would be problematic.

Considering the various characteristics outlined below, the R7400 is the default solution. However, ideally all PMT options should be evaluated and optimised against:

**Test Regime.** The photodetector efficiency (PDE) should be evaluated in the laboratory, specifically for light with a Cherenkov emission spectrum. Characterisation of the chosen devices should be measured and the dark count rate verified for the widest range of working conditions anticipated at NA62. The ability to distinguish two kaon signals close in time should also be carefully addressed,

using a pulsed laser, since this will have an impact on the choice of the front-end readout electronics for the photo-detectors. Additional tests will be needed to measure gain stability with respect to count rate, and accelerated lifetime testing will also be performed. Timing resolution measurements will also be carried out.

**Anode Current.** Although the passage of a kaon only produces an average of about 3 photons at each optical port, the high kaon rate (50 MHz) results in an illumination of 600 million photons per second. Photomultipliers are rated at a maximum anode current of about 100  $\mu$ A and a gain in the region of  $10^6$ . Coping with such high illumination implies tiling several photomultipliers together to reduce the photon flux at each device.

**Count rate per channel.** Assuming a double pulse resolution of <10 ns, a count rate per channel of less than 10 MHz is needed in order to keep the inefficiency due to pile-up below 5%. Hence, it will be necessary to divide the light between several PMT's per port. In addition, multi-anode readout will be tested as a way to reduce the count rate on each channel to a lower level.

### 1.1.8.1 Front-End electronics

The typical signal output (produced by one photon) from the baseline choice of PMT's to be used for the CEDAR is about 100  $\mu$ A peak, with a rise time of about 0.6 ns and a FWHM of about 2 ns. In the Front End Electronics, this signal will be amplified about 50 times, and then discriminated and time-stretched by a NINO ASIC to produce a LVDS signal. The NINO was designed for analogue signals from devices faster than PMT's, and requires a differential input. A suitable preamplifier/shaper board has been designed to adapt the PMT signals to the NINO input for the RICH detector. It will be placed on a PCB mounted on the PMT's themselves, and must be radiation hard<sup>2</sup>, while the rest of the electronics will be placed far enough from the beam not to require radiation hardness.

The measurement of the Time Over Threshold, implemented using the NINO chip and the time measurement of both pulse leading and trailing times in the common TDC/TEL62 readout system, will be used to extract information on the pulse amplitude, both to correct the time-slewing induced by amplitude fluctuations, and to discriminate against pile-up. Considering the PMT analogue signal to be of Gaussian shape, it can be shown that edge time and time over threshold are linearly correlated. It is possible in principle also to predict the correlation between time over threshold and amplitude.

Using 240 PMT's and a quantum efficiency of 25%, the expected kaon and photon fluxes lead to an average photo-electron rate of 3.8 MHz on a single PMT channel. The average number of detected photons per kaons is 18, while the probability of having more than one photon on a single PMT is of the order of 8% in one event and 9% in two consecutive events spaced by less than 20 ns.

---

<sup>2</sup> The expected radiation levels near the PMT's are approximately 4 Gy/year.

Considering that the PMT intrinsic time resolution is 300 ps, and that a time resolution of about 100 ps on the single kaon is needed in order to suppress the accidental background, a minimum of 9 photons need to be detected for each kaon. The dead time losses are of the order of 20 ns (11ns from NINO and 5 ns from HPTDC, and allowing for ~4ns duration of the signal). The double pulse resolution of the whole system is dominated by the electronics and is of the order of 10 ns.

### 1.1.8.2 Readout Electronics

The readout for the CEDAR will be based on the common TDC/TEL62 system. The digital signals will be sent from the front-end electronics to the readout electronics with a few metres of high-quality twisted pair cable. The times of both the leading and trailing edges of the pulse will be measured.

Concerning dead time losses, the NINO chip introduces a stretching time of 11ns, while the HPTDC has a deadtime which can be set to be 5ns but it does not contribute to the total deadtime due to the NINO mode of operation. The major limitation arises from the finite size of the HPTDC hit channel buffers , which can sustain a maximum of 40 MHz over a set of 8 channels, or a maximum of 10 MHz for a single channel, whichever is lower, on the assumption of 1 word written for each signal (or 5 MHz for 2 words).

The 16 HPTDCs in a single TDC/TEL62 boards are arranged in sets of 8 channels which share some group channel buffers. By using only 2 channels for each set (1/4 of the total number available) the rate will be reduced to a sustainable level to guarantee a small probability of hit loss, at the price of using only 32 channels per TDC board (8 channel per TDC; 128 channels per TEL62) . Hence the readout system will consist of 16 TDC boards and 2 TEL62 boards. The hit loss probability estimated in this configuration is 1%, which corresponds to a detection inefficiency per kaon of a few % for a minimum of 10 photons distributed in at least 6 spots. However, further studies are in progress to ensure that the light distribution on the spot is compatible with a rate per channel not exceeding 5 MHz.

The contribution of the readout system to the time resolution is estimated to be of the order of ~70 ps, based on the performances of a prototype system used in the RICH tests), which gives a negligible contribution when combined with the intrinsic PMT resolution of 300-400 ps.

The readout time window will be 75 ns, and an average of 4 kaons are expected to appear in such time window (with a tail up to 12 kaons). With an average of 18 hits per kaon, and 32 bit per photon, this corresponds to an average of ~288 bytes in the readout window (and a maximum of 864 bytes). Assuming a trigger rate of 1MHz, this corresponds to an average of ~0.3 GB/s of readout rate (and a maximum of 0.9 GB/s). This will be distributed on 2 TEL62.

Data arriving in an interval of 1 ms will be saved in the TEL62 buffer at any time. Given an average of 9 hits per kaon per TEL62, with 32 bit per photon and a kaon rate of 50 MHz, a maximum input of ~40 bytes is expected per kaon per TEL62, which corresponds to ~200 KB in the buffer of 1ms - well below the maximum buffer of TEL62.

The processing done in the TEL62 will include counting of the number of PMT's fired per spot and the number of fired spots, to enable the development of algorithms that use the multiplicity and the

geometry to suppress the background. It is also foreseen to record the photon times in 1ns slots inside the 75 ns readout window to allow for a precise time coincidence with the trigger signal.

## Bibliography

1. Brianti, G. and Doble, N. *The SPS North Area High Intensity Facility: NAHIF*. CERN. Geneva : s.n., 1977. SPS/EA 77-2; SPSC/T-18.